

Effects of Mg concentration on solubility and chemical state of N in N-doped MgZnO alloy

Lili Gao, Bin Yao, Bo Liu, Li Liu, Tong Yang et al.

Citation: *J. Chem. Phys.* **133**, 204501 (2010); doi: 10.1063/1.3505636

View online: <http://dx.doi.org/10.1063/1.3505636>

View Table of Contents: <http://jcp.aip.org/resource/1/JCPSA6/v133/i20>

Published by the [American Institute of Physics](#).

Additional information on *J. Chem. Phys.*

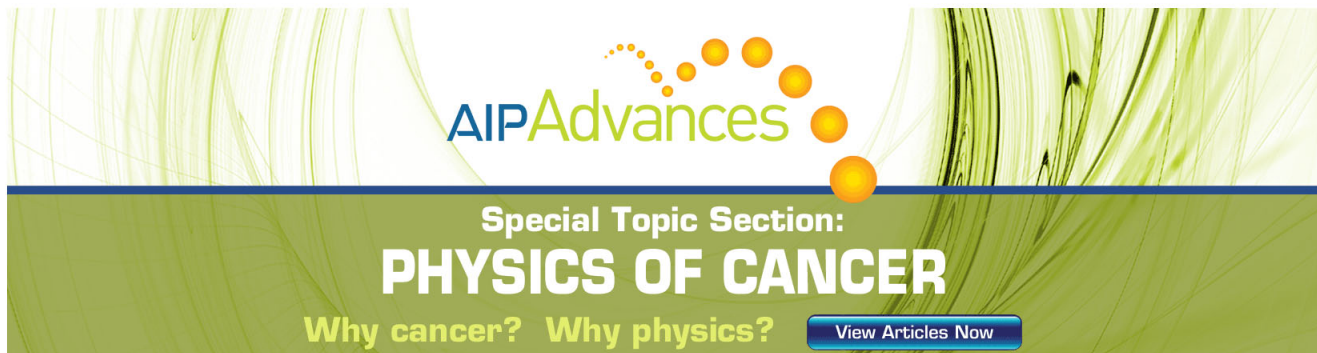
Journal Homepage: <http://jcp.aip.org/>

Journal Information: http://jcp.aip.org/about/about_the_journal

Top downloads: http://jcp.aip.org/features/most_downloaded

Information for Authors: <http://jcp.aip.org/authors>

ADVERTISEMENT



AIP Advances

Special Topic Section:
PHYSICS OF CANCER

Why cancer? Why physics? [View Articles Now](#)

Effects of Mg concentration on solubility and chemical state of N in N-doped MgZnO alloy

Lili Gao,^{1,2} Bin Yao,^{1,3,a)} Bo Liu,¹ Li Liu,² Tong Yang,¹ Bingbing Liu,¹ and Dezheng Shen³

¹State Key Laboratory of Superhard Materials and Department of Physics, Jilin University, Changchun 130023, People's Republic of China

²Department of Physics, Beihua University, Jilin 132013, People's Republic of China

³Changchun Institute of Optics, Fine Mechanics and Physics, Chinese Academy of Sciences, Changchun 130021, People's Republic of China

(Received 18 July 2010; accepted 4 October 2010; published online 24 November 2010; corrected 19 August 2011)

Solubility and chemical state of N in an N-doped $Mg_xZn_{1-x}O$ film were studied by using Raman and x-ray photoelectron spectroscopy. Three anomalous Raman peaks are observed at 272, 580, and 642 cm^{-1} , respectively, and are demonstrated to be only related to substitution of N for O site (N_O) but not to substitution of N_2 for O site ($(N_2)_O$). The solubility of the N_O is dominated by Mg concentration and chemical potentials of N and O in growth condition. The chemical state of the N can change from coexistence of $(N_2)_O$ and N_O to single $(N_2)_O$ with increasing Mg concentration. © 2010 American Institute of Physics. [doi:10.1063/1.3505636]

I. INTRODUCTION

Since band gap of MgZnO alloy with wurtzite structure is larger than that of ZnO and can be tuned by changing Mg concentration,¹ the alloy is considered as a suitable barrier layer material for preparation of ZnO-based quantum well and is investigated widely in the recent years.²⁻⁴ Now, *n*-type MgZnO with high crystal quality and various band gaps can be prepared well, but fabrication of reliable *p*-type MgZnO with good stability and electrical properties is still a difficult task and becomes bottle-neck problem obstructing application of MgZnO in optoelectronic devices. In the recent years, some research groups have made many efforts to prepare *p*-type MgZnO by using N as an acceptor dopant.⁵ However, as same as the preparation of N-doped *p*-type ZnO,^{6,7} it is also hard to fabricate reproducibly N-doped *p*-type MgZnO with low resistivity, high carrier concentration, and high mobility due to low solubility of N in MgZnO and self-compensation of $(N_2)_O$ and other native donors for N_O acceptors, where $(N_2)_O$ and N_O represent substitution of N_2 and N for O site, respectively, and are two kinds of chemical state of N in N-doped MgZnO (Ref. 5). Obviously, it is very important to increase the solubility of N_O and decrease the self-compensation of $(N_2)_O$ for fabrication of N-doped *p*-type MgZnO. Therefore, it is necessary to characterize chemical state and solubility of N in the N-doped MgZnO correctly and understand effect of Mg on the chemical state and solubility. X-ray photoelectron spectroscopy (XPS) is usually used to characterize the chemical state and the solubility of the N in the N-doped MgZnO or ZnO; however, which are demonstrated to be very difficult.

Raman spectroscopy is a versatile technique for fast and nondestructive study of dopant incorporation. Recently, this technique is used to investigate N-doped or N^+ -implanted

ZnO,⁸⁻¹³ and a number of anomalous Raman peaks are observed near 275, 504, 582, and 643 cm^{-1} besides Raman peaks of ZnO, which are considered to be related to N doping, but the origin of these peaks is still argued. In fact, the N has two chemical states of N_O and $(N_2)_O$ in N-doped ZnO, as mentioned above. If we can clarify whether the Raman peaks come from N_O or $(N_2)_O$, we can characterize expediently and exactly the chemical state of the N by Raman spectroscopy, which is important for preparation of N-doped ZnO.

In the present work, the chemical state and solubility of the N in the N-doped MgZnO film are characterized by Raman spectroscopy and XPS, effects of Mg concentration on the chemical state and solubility are investigated, and the origin of the anomalous Raman peaks is discussed.

II. EXPERIMENTAL

$Mg_xZn_{1-x}O$ films were prepared by radio frequency (rf) magnetron sputtering technique in two kinds of experimental procedures, respectively: (I) sputtering a ceramic target with a nominal component of $Mg_{0.04}Zn_{0.96}O$ using mixed gases of 99.99% pure nitrogen and argon at the flux ratio of $N_2/(N_2 + Ar)$ of 0, 1/2, 4/5, and 1, respectively, and (II) sputtering ZnO, $Mg_{0.04}Zn_{0.96}O$, and $Mg_{0.08}Zn_{0.92}O$ targets using the mixed gas at a fixed flux ratio of 4/5. In both procedures, the sputtering gases were adjusted to maintain a constant chamber pressure of 1.0 Pa, and all the $Mg_xZn_{1-x}O$ films were grown on quartz substrates for 1 h at a substrate temperature of 773 K, and then annealed for 30 min at 873 K under 10^{-4} Pa in a tube furnace.

The structures of the films were characterized by x-ray diffraction (XRD) with Cu $K_{\alpha 1}$ radiation ($\lambda = 0.15406$ nm). The composition of the $Mg_xZn_{1-x}O$ film was detected by using energy dispersive x-ray spectroscopy (EDS) and XPS. The chemical state of the N in N-doped MgZnO was characterized by XPS. Raman backscattering spectra were obtained at room

^{a)} Author to whom any correspondence should be addressed. Electronic mail: binyao@jlu.edu.cn.

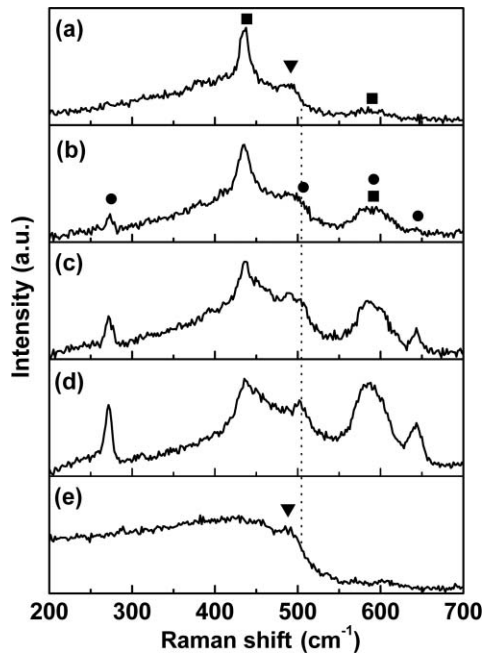


FIG. 1. Raman spectra of annealed MgZnO:N films produced by procedure (I) at various flux ratios of $N_2/(N_2 + Ar)$ of: (a) 0, (b) 1/2, (c) 4/5, (d) 1, and (e) of quartz substrate.

temperature using 514.5 nm line of an Ar^+ laser and incident power of 20 mW.

III. RESULTS AND DISCUSSION

The XRD and EDS measurements indicate that all the $Mg_xZn_{1-x}O$ films prepared in procedure (I) are MgZnO alloys with wurtzite structure and Mg content in the MgZnO films increases with increasing the flux ratio. The increment of the Mg content was interpreted in our previous literature.¹⁴ Figures 1(a)–1(d) show the normalized Raman spectra of the annealed $Mg_xZn_{1-x}O$ films grown in procedure (I) at the flux ratios of $N_2/(N_2 + Ar)$ of 0, 1/2, 4/5, and 1. Three Raman peaks are observed at about 436, 486, and 580 cm^{-1} in Fig. 1(a). The 486 cm^{-1} peak [marked by \blacktriangledown in Figs. 1(a) and 1(e)] is also found in Raman spectrum of the quartz substrate used in the present work, so it is due to Raman peak of the quartz. The 436 and 580 cm^{-1} peaks [marked by \blacksquare in Fig. 1(a)] are also observed in Raman spectrum of ZnO and are attributed to E_2^{high} and $A_1(LO) + E_1(LO)$ modes,¹⁵ respectively. This result implies that the MgZnO alloy with wurtzite structure has similar Raman spectrum to ZnO and there is no additional vibrational mode when Mg alloys with ZnO to form MgZnO.

Figures 1(b)–1(d) indicate that three additional Raman peaks are observed at about 272, 504, and 642 cm^{-1} [marked by \bullet in Fig. 1(b)] in the $Mg_xZn_{1-x}O$ films fabricated at flux ratios of 1/2, 4/5, and 1 besides the Raman peaks of E_2^{high} , A_1 , and quartz; moreover, it is also found that the intensities of the additional peaks and 580 cm^{-1} peak increase with increasing the flux ratio. Because the peak at 504 cm^{-1} partially overlaps the quartz peak, so we will not discuss it in the following. Obviously, the only difference in growth condition is

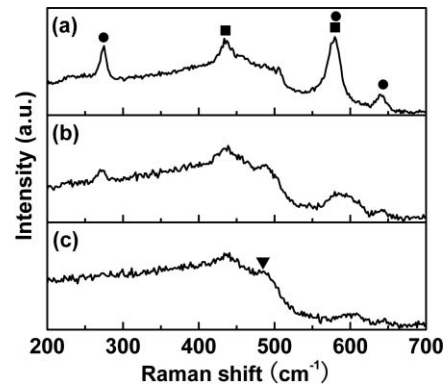


FIG. 2. Raman spectra of annealed (a) ZnO:N, (b) $Mg_{0.11}Zn_{0.89}O:N$, and (c) $Mg_{0.32}Zn_{0.68}O:N$ films produced by procedure (II).

that the sputtering gas does not contain N_2 for the $Mg_xZn_{1-x}O$ corresponding to Fig. 1(a) but for the $Mg_xZn_{1-x}O$ corresponding to Figs. 1(b)–1(d). Based on the results of Figs. 1(a)–1(d), it is deduced that N incorporates into $Mg_xZn_{1-x}O$ to form N-doped MgZnO (denoted as MgZnO:N) as the $Mg_xZn_{1-x}O$ is produced by using sputtering gas containing N_2 and that the appearance of the additional Raman peaks and increment of 580 cm^{-1} peak intensity are related to N doping in the MgZnO. Furthermore, the intensities of the three Raman peaks are in direct proportion to N concentration in the MgZnO:N. In order to confirm the deduction, the MgZnO:N were annealed for 30 min in a temperature ranging from 973 to 1173 K under 10^{-4} Pa in a tube furnace. The Raman measurement for the annealed MgZnO:N indicates that the intensity of the three Raman peaks (the Raman spectrum is not given here) decreases with increasing annealing temperature. When the annealing temperature reaches 1173 K, the 272 and 642 cm^{-1} peaks disappear. It is well known that N is in metastable thermodynamic state in the N-doped ZnO or MgZnO and will escape as the N-doped ZnO or MgZnO is annealed at temperature of above 873 K. The higher the annealing temperature, the faster the N escapes. When the temperature reaches 1173 K, all N will escape from the N-doped MgZnO. Therefore, the decrease in intensity for the three Raman peaks is due to decrease in N concentration in the MgZnO:N, which confirms above deduction. So Raman spectrum can be used to detect N doping in $Mg_xZn_{1-x}O$. Similar result is also observed in N-doped ZnO and researched wildly in the recent years,^{8–13} but origin of these Raman peaks is still argued.

It is found from the Raman and EDS measurements that both N and Mg concentrations in the MgZnO:N produced in procedure (I) increase with increasing the flux ratio, while the increase of the flux ratio means increment of N_2 content in the sputtering gas. In order to understand whether the increment of the N concentration in the MgZnO:N comes from the increase of the Mg concentration or the increase of the N_2 content in the mixed gas, one N-doped ZnO and two N-doped MgZnO were fabricated by experimental procedure (II), where the targets are ZnO and $Mg_xZn_{1-x}O$ with different Mg content and mixed gas is fixed at flow ratio of 4/5. The XRD and XPS measurements indicate that three samples are doped by N and have wurtzite structure.

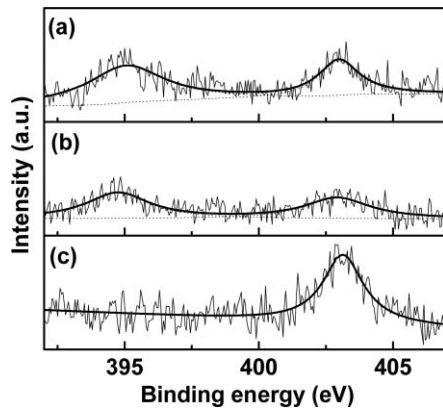


FIG. 3. XPS spectra of N_{1s} annealed (a) ZnO:N, (b) $Mg_{0.11}Zn_{0.89}O$:N, and (c) $Mg_{0.32}Zn_{0.68}O$:N films produced by procedure (II).

Figures 2(a)–2(c) exhibit normalized Raman spectra of the N-doped ZnO, $Mg_{0.11}Zn_{0.89}O$, and $Mg_{0.32}Zn_{0.68}O$ produced by procedure (II), which indicate that the intensity of 272, 642, and 580 cm^{-1} peaks decreases with increasing Mg concentration. The 272 and 642 cm^{-1} Raman peaks almost disappear as Mg concentration is 0.32, as shown in Fig. 2(c). In order to understand effect of Mg on solubility and chemical state of N as well as origin of the additional Raman peaks, XPS measurement was performed for the N-doped ZnO, $Mg_{0.11}Zn_{0.89}O$, and $Mg_{0.32}Zn_{0.68}O$.

Figures 3(a)–3(c) show the XPS spectra of N_{1s} of the N-doped ZnO, $Mg_{0.11}Zn_{0.89}O$, and $Mg_{0.32}Zn_{0.68}O$ films. Prior to the XPS measurement, all films are etched by Ar^+ ion for 120 s. Figure 3(a) shows that the N-doped ZnO has two N_{1s} peaks, located at 395 and 403 eV, respectively. Since the 395 and 403 eV are close to N_{1s} binding energy of N_O and $(N_2)_O$ in N-doped ZnO (Ref. 7), respectively, the two peaks are assigned to radiation of N_{1s} of N_O and $(N_2)_O$, respectively, which implies that the N has two chemical state of N_O and $(N_2)_O$ in the N-doped ZnO. Figure 3(b) indicates that the N also has two chemical state of N_O and $(N_2)_O$ in the N-doped $Mg_{0.11}Zn_{0.89}O$, but the N_{1s} peak intensity of the N_O becomes weaker, in comparison with the N_{1s} peak of N_O in the N-doped ZnO, implying that the N_O concentration is less in the N-doped $Mg_{0.11}Zn_{0.89}O$ than in the N-doped ZnO. However, when Mg concentration increases to 0.32, the N_{1s} peak of the N_O disappears and only N_{1s} peak of the $(N_2)_O$ is observed, as shown in Fig. 3(c), implying that there is no N_O in the N-doped $Mg_{0.32}Zn_{0.68}O$. Figure 3 indicates that the N_O concentration decreases with increasing Mg concentration in the N-doped MgZnO produced at a fixed flux ratio. Based on the results of Figs. 2 and 3, three important conclusions are obtained: (1) Mg can change chemical state of N in the N-doped MgZnO at a fixed flux ratio, (2) the additional Raman peaks observed in N-doped ZnO and MgZnO are only related to N_O but not to $(N_2)_O$, and (3) N_O solubility in N-doped MgZnO produced in procedure (II) decreases with increasing Mg concentration.

It is worth noting that the third conclusion seems to be contradictory to the results reported in our previous literatures¹⁶ and observed in the N-doped MgZnO produced by procedure (I).

TABLE I. Formation energy $\Delta E(N_O)$ for N-doped $Mg_{0.25}Zn_{0.75}O$ and N-doped ZnO.

mNN	$\Delta E(N_O)$
3NN	$2.509 - \mu_N + \mu_O$
2NN	$2.054 - \mu_N + \mu_O$
1NN	$1.623 - \mu_N + \mu_O$
0NN	$1.215 - \mu_N + \mu_O$
ZnO	$1.113 - \mu_N + \mu_O$

Many research literatures on N-doped ZnO indicate that the solubility and chemical states of N in ZnO are related to the stoichiometry of ZnO and chemical potentials of N and O. For example, N incorporates easily into ZnO under O-poor condition. However, for N-doped MgZnO, the solubility and chemical states of N are not only influenced by the stoichiometry and the chemical potentials of the N and O, but also by Mg concentration; and even the Mg concentration seems to have dominant influence under some conditions based on the present experimental results mentioned above. In order to understand the effect of Mg on N_O solubility, our groups have previously calculated the formation energy of N_O in N-doped ZnO and $Mg_{0.25}Zn_{0.75}O$ disordered alloy using first-principles calculation and results are listed in Table I.¹⁶ The formation energy $\Delta E(N_O)$ can be written by

$$\Delta E(N_O) = E_{ZnO}(\text{or } E_{MgZnO}(\text{mNN})) - \mu_N + \mu_O, \quad (1)$$

where E_{ZnO} and $E_{MgZnO}(\text{mNN})$ are formation energy of N_O in ZnO and $Mg_{0.25}Zn_{0.75}O$ having m Mg ions at nearest neighbor site of N_O when $-\mu_N + \mu_O = 0$, respectively, and μ_N and μ_O are chemical potential of N and O, respectively. Table I shows that the first term in Eq. (1) increases with increasing the number of Mg ion at nearest neighbor site of N_O , which implies that N_O is easier to bind with Zn than Mg and the $E_{MgZnO}(\text{mNN})$ increases with increasing Mg concentration. The μ_N and μ_O are related to growth condition of the films, and increase in μ_N or decrease in μ_O can make the N_O solubility in the MgZnO increase.

For $Mg_xZn_{1-x}O$:N produced by procedure (I), the Mg concentration increases only from 0.06 to 0.17 with increasing the flow ratio from 0 to 1. The Mg concentration is too small to have enough possibility to bind with N_O , resulting in that the $E_{MgZnO}(\text{mNN})$ increases little with increasing the flux ratio. On the other hand, since N content in the mixed gas increases and O content decreases with increasing the flux ratio, the μ_N increases but μ_O decreases greatly with increasing the flux ratio. Therefore, the change of the $\Delta E(N_O)$ is dominated by change of μ_N and μ_O . Based on Eq. (1) and above discussion, it is deduced that the $\Delta E(N_O)$ decreases with increasing the flux ratio, which is favorable to incorporation of N_O into MgZnO. In addition, it is also found that O concentration in MgZnO decreases with increasing the flux ratio, which is also favorable to N_O doping in the MgZnO. According to the above discussion, it is deduced that the increment of the N_O solubility in the $Mg_xZn_{1-x}O$:N produced in procedure (I) is mainly due to increase in μ_N , decrease in μ_O and O concentration, and the effect of Mg on the N_O solubility is little.

However, for the N-doped $\text{Mg}_x\text{Zn}_{1-x}\text{O}$ produced in procedure (II), it is found from the EDS measurement that the atomic ratio of O to (Mg + Zn) deviates from the stoichiometry and decreases from 0.783 to 0.668, as the Mg concentration increases from 0 to 0.32, which implies that the O vacancies of the $\text{Mg}_x\text{Zn}_{1-x}\text{O}:\text{N}$ increases with increasing Mg concentration. However, the XPS and EDS measurements indicate that the N_O solubility does not increase with increasing O vacancies but decreases with increasing Mg concentration, which means that the N_O solubility is not dominated by stoichiometry but the Mg concentration. In fact, the μ_N and μ_O change little in procedure (II) due to fixed flux ratio, so the $\Delta E(\text{N}_\text{O})$ is dominated by the first term of Eq. (1). Since the $\Delta E(\text{N}_\text{O})$ increases when the Mg and N_O become the nearest neighbors, as indicated in Eq. (1), the amount of N_O incorporated into the $\text{Mg}_x\text{Zn}_{1-x}\text{O}$ should decrease when Mg concentration increases to avoid increase in the $\Delta E(\text{N}_\text{O})$, that is, the N_O solubility of the $\text{Mg}_x\text{Zn}_{1-x}\text{O}$ is dominated by the Mg concentration and decreases with increasing Mg concentration.

In addition, since the amount of N and O is fixed in procedure (II), the decrease in N_O solubility induced by the increase in the Mg concentration implies that more N atoms or molecule will remain in the growth ambient and react with O to form NO or NO_2 . For the NO or NO_2 will be expelled soon by pump, the amount of the O in the growth ambient goes down, leading to a decrease in the O concentration in the N-doped $\text{Mg}_x\text{Zn}_{1-x}\text{O}$ with increasing Mg concentration, in agreement with the EDS measurement results. The agreement also confirms that the three conclusions mentioned above are reliable and the suggested mechanism of the effect of Mg on the solubility and chemical states of the N is reasonable.

IV. CONCLUSION

Effects of Mg on solubility and chemical state of N in the N-doped $\text{Mg}_x\text{Zn}_{1-x}\text{O}$ thin films were investigated by Raman spectroscopy and XPS. Three characteristic Raman peaks related to N doping are observed in the N-doped $\text{Mg}_x\text{Zn}_{1-x}\text{O}$ at 272, 580, and 642 cm^{-1} , respectively, and are demonstrated to be only related to N_O but not to $(\text{N}_2)_\text{O}$. The intensity of these Raman peaks is in direct proportion to N_O concentration in the N-doped $\text{Mg}_x\text{Zn}_{1-x}\text{O}$. The solubility of N_O in the N-doped $\text{Mg}_x\text{Zn}_{1-x}\text{O}$ is affected by the number of Mg at nearest neighbor site of N_O as well as μ_N and μ_O . The solubility decreases with increasing Mg concentration and μ_O but in-

creases with increasing μ_N . The chemical state of N in the $\text{MgZnO}:\text{N}$ is influenced by Mg concentration when μ_N and μ_O is fixed and can be changed from coexistence of N_O and $(\text{N}_2)_\text{O}$ in the $\text{MgZnO}:\text{N}$ with low Mg concentration to single $(\text{N}_2)_\text{O}$ in the $\text{MgZnO}:\text{N}$ with high Mg concentration.

ACKNOWLEDGMENTS

This work is supported by the Key Project of National Natural Science Foundation of China under Grant No. 50532050, the “973” program under Grant No. 2006CB604906, the Innovation Project of Chinese Academy of Sciences, the National Natural Science Foundation of China under Grant Nos. 6077601, 60506014, 10674133, 60806002, and 10874178, National Found for Fostering Talents of basic Science under Grant No. J0730311. Swedish Research Links via VR.

- ¹A. Ohtomo, M. Kawasaki, T. Koida, K. Masubuchi, and H. Koinuma, *Appl. Phys. Lett.* **72**, 2466 (1998).
- ²S. Choopun, R. D. Vispute, W. Yang, R. P. Sharma, T. Venkatesan, and H. Shen, *Appl. Phys. Lett.* **80**, 1529 (2002).
- ³W. I. Park, G.-C. Yi, and H. M. Jang, *Appl. Phys. Lett.* **79**, 2022 (2001).
- ⁴Y.-I. Kim, K. Page, A. M. Limarga, D. R. Clarke, and R. Seshadri, *Phys. Rev. B* **76**, 115204 (2007).
- ⁵Z. P. Wei, B. Yao, Z. Z. Zhang, Y. M. Lu, D. Z. Shen, B. H. Li, X. H. Wang, J. Y. Zhang, D. X. Zhao, X. W. Fan, and Z. K. Tang, *Appl. Phys. Lett.* **89**, 102104 (2006).
- ⁶E.-C. Lee, Y.-S. Kim, Y.-G. Jin, and K. J. Chang, *Phys. Rev. B* **64**, 085120 (2001).
- ⁷C. L. Perkins, S.-H. Lee, X. Li, S. E. Asher, and T. J. Coutts, *J. Appl. Phys.* **97**, 034907 (2005).
- ⁸A. Kaschner, U. Haboeck, M. Strassburg, M. Strassburg, G. Kaczmarczyk, A. Hoffmann, C. Thomsen, A. Zeuner, H. R. Alves, D. M. Hofmann, and B. K. Meyer, *Appl. Phys. Lett.* **80**, 1909 (2002).
- ⁹C. Bundesmann, N. Ashkenov, M. Schubert, D. Spemann, T. Butz, E. M. Kaidashev, M. Lorenz, and M. Grundmann, *Appl. Phys. Lett.* **83**, 1974 (2003).
- ¹⁰J. Sann, J. Stehr, A. Hofstaetter, D. M. Hofmann, A. Neumann, M. Lerch, U. Haboeck, A. Hoffmann, and C. Thomsen, *Phys. Rev. B* **76**, 195203 (2007).
- ¹¹J. B. Wang, H. M. Zhong, Z. F. Li, and W. Lu, *Appl. Phys. Lett.* **88**, 101913 (2006).
- ¹²L. Artus, R. Cusco, E. Alarcon-Llado, G. Gonzalez-Diaz, I. Martil, J. Jimenez, B. Wang, and M. Callahan, *Appl. Phys. Lett.* **90**, 181911 (2007).
- ¹³F. Friedrich, M. A. Gluba, and N. H. Nickel, *Appl. Phys. Lett.* **95**, 141903 (2009).
- ¹⁴C. X. Cong, B. Yao, G. Z. Xing, Y. P. Xie, L. X. Guan, B. H. Li, X. H. Wang, Z. P. Wei, Z. Z. Zhang, Y. M. Lv, D. Z. Shen, and X. W. Fan, *Appl. Phys. Lett.* **89**, 262108 (2006).
- ¹⁵Y.-I. Kim, S. Cadars, R. Shayib, T. Proffen, C. S. Feigerle, B. F. Chmelka, and R. Seshadri, *Phys. Rev. B* **78**, 195205 (2008).
- ¹⁶Y. Q. Gai, B. Yao, Z. P. Wei, Y. F. Li, Y. M. Lu, D. Z. Shen, J. Y. Zhang, D. X. Zhao, X. W. Fan, J. B. Li, and J.-B. Xia, *Appl. Phys. Lett.* **92**, 062110 (2008).